平成 29 年度

三重大学大学院　生物資源学研究科

修士論文

2016 年 1 月の日本の大寒波に伴う
北極振動の急激な極性反転と北極海氷の減少

Climate and Ecosystems Dynamics Division Graduate school of Bioresouces

Mie University

516M203

Taishi Saka

Supervisor: Prof. Yoshihiro Tachibana

Abstract

From December 2015 to January 2016, was greatest reversal ever recorded statistical for Arctic Oscillation (AO). But, the Arctic Oscillation in December had a large standard deviation of $+3\sigma$, after that was turned -3σ in next month. According to variation of Arctic Oscillation, East Asia caught big cord surge in January 2016, was the greatest snowfall ever recorded in Okinawa and Kagoshima of Japan. Moreover, the Barents and Kara sea ice decrease in January recorded the highest value in the past. However, there has no study that tried to attempt the relationship between Arctic Oscillation of large reversal and decreased sea ice in Barents and Kara Sea. Using a reanalysis dataset, sea ice retreats due to warm air advection and wind stress to Barents and Kara Sea in the process that Arctic Oscillation turned to positive, forcing excellence barotropic ("blocking") anticyclone in the upper layer from heat source response to atmosphere, which jet wave becomes big meandering, have discovered atmospheric sea ice delay interaction in which Arctic Oscillation turned to negative.

As a result, in late January 2016, steady rossby wave response that propagated from the North Atlantic to East Asia caused a big cold surge to Japan.

In order to support above mechanism, we considered steady atmospheric response to the diabatic heating anomalies over the Barents and Kara Sea with a linear baroclinic model. It formed an outstanding blocking high in the Barents and Kara Sea, and the results showed that the wave train structure of the atmosphere was similar to the reanalysis data.

Contents

1. Introduction

In recently years with global warming, the arctic region shows a larger temperature rise tendency than other regions, and the arctic sea ice loss especially brings about remote influences due to atmospheric wave activity, affecting the mid-high latitude climate is suggested (Honda et al., 2008). The influence of the decrease of sea ice in the arctic sea has been pointed out not only in small areas but also on large scale fields. In particular, the climate change in the winter northern hemisphere accompanying the rapid decrease of sea ice in recent years compared to before 2000 is related to the arrival of cold on Eurasian continent (Mori et al., 2014). Changes in these winter climate may be explained by Arctic Oscillation (http://www.bio.mie-u.ac.jp/kankyo/shizen/lab1/earth/AOindex_index.html ;Fig. 1). It is known the field showing the AO positive phase is a warm winter tendency in East Asia and the cold winter trend in the negative phase.

From December 2015 to January 2016, AO shows rapid reversal. When attention was show from December to February, the case where polarity reversal occurred in one month has never been statistical since 1980. In this reversal, the AO negative phase resulted in the first cold surge in East Asia in the history of observation. In Okinawa of Japan the first time in observation history, in Kagoshima prefecture brought about snowfall for 115 years (http://www.data.jma.go.jp/gmd/extreme/kaigi/2016/0307_teirei/h27gidai4-2.pdf).

Also, the sea ice of the Barents and Kara Sea (BKS) near the Arctic in January 2016 showed the past minimum value (http://nsidc.org/arcticseaicenews/2016/03/another-record-low-for-arctic-sea-ice-maximum-winter-extent/). December 2015 through February 2016, the Arctic in winter recorded the hottest in observation history (Cullather et al., 2016). Studies based on observational data analysis and numerical model experiments show that the negative phase of the Arctic oscillation is more likely to appear with the reduction of the sea ice in the Arctic Ocean (Jaiser et al., 2012; King et al., 2015; Nakamura et al., 2015). This is because planetary wave excited from the troposphere due to the late autumn decrease of sea ice propagate upwards, the stratospheric polar night jet decelerates. Suddenly stratosphere warming due to the deceleration of the polar night jet, the influence propagates downward and vertically joins, and represents the negative phase signal of AO in the troposphere. The mechanism to the AO negative phase through the stratosphere above is not only discussion of reanalysis data, but also discussion using numerical model experiments is thriving. In various studies, it is known that the sea surface temperature and sea ice are determined by AGCM (Analysis and atmospheric General Circulation Mode) experiment and the response due to the decrease of the sea ice in the Arctic Ocean represents the AO negative phase (Kim et al., 2014). It is also said that the reduction of sea ice from the summer to the autumn would be affect time development in winter.

However, in the past research, the planetary wave caused by the late autumn sea ice reduction propagates through the stratosphere to the lower troposphere due to time evolution, but no studies have discussed the AO negative phase by only the tropospheric variation. In this study, we focused on the sea ice reduction in the BKS, which showed the highest decrease in the past, and investigated the sort term mechanism of turning from AO positive phase to AO negative phase from fluctuations only in the troposphere.

2. Data and Analysis methods, Model

Data

In this study, we used the Japanese 55-year ReAnalysis (JRA-55) daily and monthly means dataset (Kobayashi et al., 2015).

We obtained Sea Surface Temperature (SST) and sea ice concentration data from the daily 0.25°NOAA Optimum Interpolation SST V2 (Reynolds et al., 2002).

Analysis Methods

We defined BKS as 70°N to 78°N, 20°E to 80°E.

Ogi et al (2004) identified seasonal variations in the Northern Hemisphere annular mode from 1958 to 2002 by performing an empirical orthogonal function (EOF) analysis.

They applied the EOF to a temporal covariance matrix of geopotential height fields for individual calendar months using the zonally averaged monthly geopotential height field from 1000 to 200 hPa for the area poleward of 40°N. In this study, we used the SV NAM index as defined by Ogi et al (2004), and all references to the AO index in this paper mean the SV NAM index. The SV NAM indices was available on the web at http://www.bio.mie-u.ac.jp/kankyo/shizen/lab1/earth/AOindex_index.html.

To analysis the propagation of anomaly planetary wave troposphere, we used the EP flux and its divergence on a latitude-height cross section as described under equations. Its meridional componentF_{ϕ}, component F_p, and horizontal divergence $\nabla \cdot \mathrm{F}$ were expresses in spherical geometry as

$$F_{\phi} = -r_0 cos\phi\overline{u'v'},$$

$$F_p = -f r_0 cos\phi\, \overline{v'\theta'}/(\partial\theta/\partial p),$$

$$\nabla \cdot \mathrm{F} = \frac{1}{r_0 cos\phi}\frac{\partial}{\partial\phi}\left(F_{\phi}\cos\phi\right) + \frac{\partial}{\partial p}(F_p),$$

Where r_0 denotes the Earth’s radius, f denotes the Coriolis parameter, u and v represent the zonal and meridional components of wind, and θ represents the potential temperature.

Model

Linear Baroclinic Model (LBM) developed by Watanabe and Kimoto (2000), was used to examine steady atmospheric response to a heating anomaly over targeted areas. The dynamical frame work was simplified in LBM by removing nonlinearlity in the dynamical atmosphere, the results would be much easily interpreted. The horizontal resolution is about 2.8°, the vertical resolution is 20 layers, and the top end is 5 hPa. The initial value was climate mean field calculated using December average JRA-55 reanalysis data from 1980 to 2014. An average value from 30 days to 50 days after model execution was used. Also the center and the lowest layer indicate the maximum value.

3. Result

3.1 In January 2016 big cold surge and warm winter in 2015 over the East Asia

We first investigated the mid-latitude climate of the early winter and East Asia. In general, East Asia in winter is known to get colder with the progression of season (Fig. 2a). But, December, 2015 and January, 2016 was an abnormal year (Fig. 2b). It shows monthly mean geopotential height and horizontal wind anomaly at 925 hPa in December, and January (Fig.3a and Fig 3b). December shows the air pressure arrangement an anticyclone area in the northeast and a cyclone area in the southwest, January represents the opposite. Monthly mean deviation from climatology temperature in December was +2.49℃, and January was -1.17℃. In the East Asia of January 25, it recorded -6℃ compared with annual event, showing an abnormity temperature (Fig. 2b). And, it has shown wave train structure crossing Eurasia on the upper layer 300 hPa from January 21, 2016 to 25 (Fig. 4).

On the other hand, the AO shows the mid-latitude climate during the winter indicates a positive in December and a negative in January. Positive AO in December was accompanied with cyclone anomaly in the Arctic and anticyclone anomaly in the mid-latitudes. However, negative AO in January indicated anticyclone anomaly in the Arctic and cyclone anomaly in the mid-latitudes. Cold polar air then accumulates near the surface and impacts lower-latitude regions, including East Asia (Takaya and Nakamura 2005).

As a result, it suggested that the above cold surge can be explained in January.

3.2 Reduction of sea ice in Barents and Kara Sea

At first, the sea ice concentration and SST of the anomaly from the daily climate values in BKS from December 1, 2015 to January 31, 2016 were investigated. In the early winter climate, it was known that the sea ice gradually increases as the season progresses, and SST relatively decreases. But, in the winter of 2015/2016 was contrary for the above sentence, sea ice decreased in late December, the relative SST indicated rise (Fig. 5). Especially, from December 20, it can be seen that sea ice was rapidly decreasing.

We examined how the mechanism of the reduction sea ice in the BKS. In order to investigate the mechanism of sea ice reduction, change of atmospheric temperature

$$\frac{\partial T}{\partial t} = \frac{DT}{Dt} - \boldsymbol{V} \cdot \nabla T - \omega \frac{\partial T}{\partial p} \quad \cdots (1)$$

Where, ω, T and ∇ are the horizontal wind vector, vertical p-velocity, air temperature and isobaric gradient operator, respectively. The right side of this equation shows a warming or cooling of the air mass due to diabatic absorption (first term), horizontal thermal advection (second term), and vertical-motion (third term).

We examined horizontal temperature advection term, expanded as follows:

$$-\boldsymbol{V} \cdot \nabla T = -\boldsymbol{V_C} \cdot \nabla T_C - \boldsymbol{V_C} \cdot \nabla T_a - \boldsymbol{V_a} \cdot \nabla T_C - \boldsymbol{V_a} \cdot \nabla T_a \quad \cdots (2)$$

The subscript “a” refers to the anomaly in 2015 and 2016, and “c” refers to the climatic values. We estimated respectively terms at 900hPa. In this study, $-\boldsymbol{V_a} \cdot \nabla T_C$ was adopted because it was a dominant term compared to others. At 900 hPa field, warm air advection was shown mainly in the Kara Sea from December, 1 to 21 (Fig. 6). The horizontal wind in the above same period was superior to anomaly wind in the southerly wind.

Also, it was suggested that sea ice has decreased due to wind stress caused by atmospheric circulation.

On the other hand, sea ice reduction may be caused by wind stress. The figure shows the wind and sea ice anomaly of BKS on December 16-20 and 21-25 (Fig. 7a and Fig 7b). In addition, the lines show an ice margin of 0.4 at the first and last days of both periods. The south wind anomaly was shown in both periods. The edge of the sea ice has retreated to the polar side due to time development, but it is conceivable that southerly wind is remarkable compared with the year.

These suggest that warm air advection and sea ice reduction due to wind stress.

3.3 Heat source response to the atmosphere by the ocean

In this case, since the reduction of sea ice in the BKS was more significant than usual, the turbulent heat flux due to the exposure of the sea was investigated. Turbulent heat flux used in this study was calculated by sum of sensible heat flux and latent heat flux. Turbulent heat flux for area averaged of the BKS during the period from December 1 to January 31 tends to decrease with the progression of the season (Fig. 8 Green line).

The sea ice concentration and the turbulent heat flux for the 5day average from December 16 to 20 are due to the decrease of sea ice over the BKS, from the ocean to the atmosphere in the corresponding heat source was transported (Fig. 7a shows shade). Heat transportation from ocean to atmosphere accompanying the sea ice decrease was continued until January 14 of the next month (Fig. 8 Purple bar).

We investigated the heat source response of the ocean to the atmosphere due to the decrease in BKS sea ice. As the AO reached its maximum on December 22, sea ice decreased in the BKS, and there was heat transportation from the sea to the atmosphere due to the exposure of the sea (Fig. 5 and Fig. 8). Heat forcing from the lower layer of the BKS was thought to be due to non-adiabatic heating in latent heat and sensible heat, which was caused by the sea ice distribution. According to Honda et al., 2009, it was shown by reanalysis and model experiments that the thermal response from ocean to atmospheric side caused by the decrease in sea ice for the BKS in late autumn affects the cooling in winter Eurasia.

As a result, it can be confirmed that the geopotential height anomaly at 1000 hPa from December 21 to late was a cyclone anomaly in the BKS (Fig. 9).

The geopotential height on December 21 to 25 was average at 70°to 80° (Fig. 10). The horizontal and vertical component arrows of the wave activity flux were put on anomaly field. Upward propagation of the stationary rossby wave transmitted from the lower to the upper was locate in BKS. At the point of upward propagation, it was indicated cyclone anomaly.

Next, we investigated the seasonal progress of the large-scale caused by the heat forcing of the BKS. It showed anomaly from zonal mean in the zonal wind in December 26 to 30 (Fig. 11).

Therefore, it was put on horizontal and vertical vector anomaly of above same period EP-Flux, which showed divergence and convergence in contour. From north latitude 60°to 70°, troposphere was eastward wind anomaly, and EP-Flux propagated from lower layer to upper layer. In the TEM equation system, when EP-Flux decelerating, it was known that zonal mean wind decreases due to vortex. After that, the deceleration of the jet stream becomes prominent. Moreover, we find out where troposphere was attributed to EP-Flux that propagated form lower layer to upper layer.

For poleward heat flux propagation term, expanded as follows:

$$V'T' = V_c'T_c' + V_c'T_a' + V_a'T_c' + V_a'T_a' \quad \cdots (3)$$

The subscript "a" refers to the anomaly in 2015 and 2016, and "c" refers to the climatic values, single quotation indicates the deviation from zonal mean. The right side of this equation shows that contribute by climatology planetary wave (first term), climatology planetary wave and interaction of wave propagation (second and third term), contribute by wave propagation (fourth term). When the poleward heat flux in the above same period was determined, it was positive in the BKS (Fig. 12a to Fig. 12d). This was a vertical component of EP-Flux, and since it was positive which conceivable that the effect of the vortex from lower layer to upper layer.

As a result, it can be suggested that tropospheric jet decelerated due to heat forcing in the BKS. This indicates that tropospheric jet stream was meandering. The reason for jet meandering can be confirmed on the 300 hPa in upper troposphere.

The actual value and anomaly of the 10 day average in geopotential height on the 300 hPa from December 31 to January 9 was shown figure 13. According to Yamazaki et al (2013), dipole type blocking high pressure was seen in upper layer of the BKS. This blocking high was stationary even when the season advanced. In the case where the AO shows a positive value, the tropospheric jet was excellence, and blocking high exists as stated, so that this becomes barrier and the jet may meander in due course.

Blocking high on BKS after the above period gradually shifted to the Arctic side as AO turned to its minimum value (Fig. 14). The field showing the anticyclone anomaly at the center of the Arctic is similar to the field of the AO negative phase. From these results, the blocking high developed on BKS in the AO positive phase period shifted to the extreme side due to time evolution and became the AO negative phase field representing the anticyclone in the North Pole.

Consequently, the index of AO reversed and showed a negative value.

3.4 Steady atmospheric responses to forcing over the Barents and Kara Sea

To elucidate the impact of the BKS heating anomaly on the atmospheric circulation, steady atmospheric response was calculated by the LBM. The reason for giving a heat source to the above place is to correspond to the melted sea ice of the BKS. The places given the non-adiabatic heating anomaly are shown in Fig 15. The vertical heating anomaly was given from the bottom layer to the 0.5σ layer (Fig. 16). Turbulent heat flux is the mean value of the geopotential height at 300hPa from December 21 to January 10, which is the period of significant positive anomaly (Fig. 17). Compared to LBM experiment results (Fig. 18), high similarity of anomaly between BKS and Far East and Arctic region could be confirmed.

Therefore, formation of blocking high accompanying heat source response on BKS was confirmed.

4. Discussion and Conclusion

In this study, we discovered mechanism which caused inversion AO during a month from December 2015 to January 2016. When AO moved a positive maximum late in December, BKS sea ice rapidly decreases. In the climatology of BKS sea ice increased with seasonal evolution. In the winter of 2015/2016, sea ice in BKS was rapidly decreased compared to the climatology, it indicated large value in recent years.

The sea ice rapidly decrease in late December was caused by the warm air advection to the BKS which started from the first half of December. The $-\boldsymbol{V_a} \cdot \nabla T_C$ term of the horizontal temperature advection was warm air advection mainly in the BKS as the AO reached the maximum value. This may be because the wind from the continent to the sea was larger than normal. In addition, wind stress due to south wind anomaly suggested sea ice retreat to the polar region.

As a result, the sea was exposed as the sea ice in the BKS rapidly declined in late December.

Due to the exposure of the sea, the atmosphere and the ocean have large thermal contrast, so it was found that the heat was transported from the sea to the atmosphere. There was a day when the difference was about 13° at maximum (Fig. 19). The above heat transport was in the same with seasonal progress of sea ice reduction. This was considered to be that warm air advection and wind stress occurred on the BKS in the process where AO turned to the maximum, the sea ice decreased, and it was strengthened with the heat source response.

Next, the behavior of the stationary rossby wave accompanied by the heat source response of BKS was the 5day mean from December 21 to 25, the steady rossby divergence was seen mainly in BKS. A similar response was seen above response from December 26 to 30. Examining the behavior to the atmospheric accompanying the stationary rossby wave response in the BKS, it caused superior blocking high to the upper layer. This blocking high shows stretching anomaly from lower layer to upper layer, it lasted until the middle of January.

In generally, when AO was a positive, it shows cyclone anomaly centering on the north polar, and tropospheric jet was known to be westerly wind anomaly at mid latitude.

In the other hands, when the AO was a negative, it shows the opposite anomaly from the above, and the jet indicates the easterly wind anomalous. It was a zonal mean zonal wind from December 26 to 30, shows an easterly anomaly wind, and tropospheric jet was deceleration. Since EP-Flux propagates upward from the troposphere lower layer and the convergence of flux was observed at the point where the easterly wind anomaly was shown on the 300 hPa, it was conceivable that the jet decelerated due to the effect of disturbance. When considering which part of EP-Flux propagation upward, the polar heat flux from December 26 to 30 was positive in the BKS. Because of the north wind anomaly and low temperature anomaly, since the polar heat flux shows a positive value, it was understood that energy was propagated vertically upward in the BKS. It was thought that energy was propagated upward by heat source response due to sea ice reduction and contributes to deceleration of tropospheric jet.

Consequently, it was suggested that the tropospheric jet decelerated with the development of blocking high on the BKS from December 26 to 30. After that, the blocking high on BKS shifted to the Arctic side and became a place showing AO negative phase.

Therefore, in the process that AO turns to positive sea ice the BKS decreases due to warm air advection and wind shear, blocking high was formed by the heat source response due to exposure of the sea, as a result, AO was decelerated as the tropospheric jet decelerates, it was thought that turned to negative.

To support these analytical results, the mechanism of blocking high development by the heat source response in LBM experiment over the BKS was examined.

5. Reference

Cullather, R. I., Y. Lim, L. N. Boisvert, L. Brucker, J. N. Lee, and S. M. J. Nowicki 2016b: Analysis of the warmest Arctic winter 2015–2016, Geophys. Res. Lett., **43**, 808–816, doi:10.1002/2016GL071228.

Edmon, H. J., B. J. Hoskins, and M.E. Mclntyre 1980: Eliassen-Palm cross sections for the troposphere, *J.Atmos. Sci.,* **37**, 2600-2616.

Honda, M., J. Inoue and S. Yamane, 2009: Influence of low Arctic sea-ice minima on anomalously cold Eurasian winters. *Geophys. Res. Lett*, **36**, L08707, doi:10.1029/2008GL037079.

Inoue, J., and T. Kikuchi, 2007: Outflow of summertime Arctic sea ice observed by ice drifting buoys and its linkage with ice reduction and atmospheric circulation patterns. *J. Meteor. Soc. Japan.,* **85**, 881-887.

Jaiser, R., Dethloff, K., Handorf, D., Rinke, A. and Cohen, J. 2012: Planetary- and baroclinic-scale interactions between atmospheric and sea ice cover changes in the Arctic. *Tellus A* **64**, 11595. DOI: 10.3402/tellusa.v64i0.11595.

Kim, B.-M., et al. 2014: Weakening of the stratospheric polar vortex by Arctic sea-ice loss, *Nat. Commun.,* 5, 4646, doi:10.1038/ncomms5646.

King, M. P., M. Hell, and N. Keenlyside 2015: Investigation of the atmospheric mechanisms related to the autumn sea ice and winter circulation link in the Northern Hemisphere, *Clim. Dyn.,* doi:10.1007/s00382-015-2639-5.

Kobayashi, S., Y. Ota, Y, Harada, A. Ebita, M. Moriya, H. Onoda, H. Kamahori, C. Kobayashi, H. Endo, K. Miyaoka, and K. Takahashi, 2015: The JRA-55 Reanalysis: General Specifications and Basic Characteristics, *J. Meteor. Soc. Japan*., **93**, 5-48.

Mori, M., Watanabe, M., Shiogama, H., Inoue, J. & Kimoto, M., 2014: Robust Arctic sea-ice influence on the frequent Eurasian cold winters in past decades. *Nature Geoscience.,* **7**, 869- 873.

Nakamura, T., K. Yamazaki, K. Iwamoto, M. Honda, Y. Miyoshi, Y. Ogawa, J. Ukita, 2015: A negative phase shift of the winter AO/NAO due to the recent Arctic sea-ice reduction in late autumn. *J. Geophys. Res.,* **120,** 3209-3227.

Ogi, M., K. Yamazaki, and Y. Tachibana, 2004: The summertime annular mode in the Northern Hemisphere and its linkage to the winter mode. *J. Geophys. Res.,* **109**, D20114, doi:10.1029/ 2004JD004514.

Ogi, M., and Ignatius G. Rigor, 2013: Trends in Arctic sea ice and the role of atmospheric circlulation. *Atmos. Sci. Let.,* **14**, 97-101.

Reynolds, R. W., N. A. Rayner, T. M. Smith, D. C. Stokes, and W. Wang, 2002: An improved in situ and satellite SST analysis for climate. *J. Climate.,* **15**, 1609-1625.

Sato, K., Inoue, J. & Watanabe, M.2014: Influence of the Gulf Stream on the Barents Sea ice retreat and Eurasiancoldness during early winter,*Environ. Res. Lett*., **9,** 084009-084017.

Serreze, M. C., and J. Stroeve, 2015: Arctic sea ice trends, variability and implications for seasonal ice forecasting. *Philos. Trans. Roy. Soc. A.,* **373**, 2045, doi:10.1098/rsta.2014.0159.

Takaya, K and Nakamura, H 2001: A formulation of a phase-independent wave-activity flux for stationary and migratory quasigeostrophic eddies on a zonally varying basic flow, *J. Atmos. Sci*., **58**, 608-627.

Takaya, K and Nakamura, H 2005: Geographical dependence of upper-level blocking formation associated with intraseasonal amplification of the Siberian high, *J. Atmos. Sci.,* **62**, 4441-4449.

Thompson, D. W. J., and J. M. Wallace, 1998: The Arctic oscillation signature in the wintertime geopotential height and temperature fields. *Geophys. Res. Lett.,* **25**, 1297-1300.

Watanabe, M. and F.-F. Jin, 2003: A moist linear baroclinic model: Coupled dynamical-convective response to El Nino. *J.Climate.,* **16**, 1121-1139.

Yamazaki and Itoh 2013a,b: Vortex-vortex interactions for the maintenance of blocking. *J. Atmos. Sci.,* **70**, 725-742 & 743-766.

6. Acknowledge

I would like to thank Prof Yoshihiro Tachibana who provided carefully considered feedback and valuable comments.

I also owe a very important debt to Assoc. prof Kazuaki Nishii who gave me deeply comments and warm encouragements.

I express gratitude to associate Prof Yoshihiro Iijima. He taught me the knowledge of reinforcement layer physical process.

Koji Yamazaki taught me the knowledge of the physics. I appreciate to him.

Masayo Ogi thank you for your kind attention, including detailed analysis suggestions and email exchange.

Many professors of Geosystem Science, Graduate school of Bioresources, Mie University advised me. I thank that very much.

7. List of figures

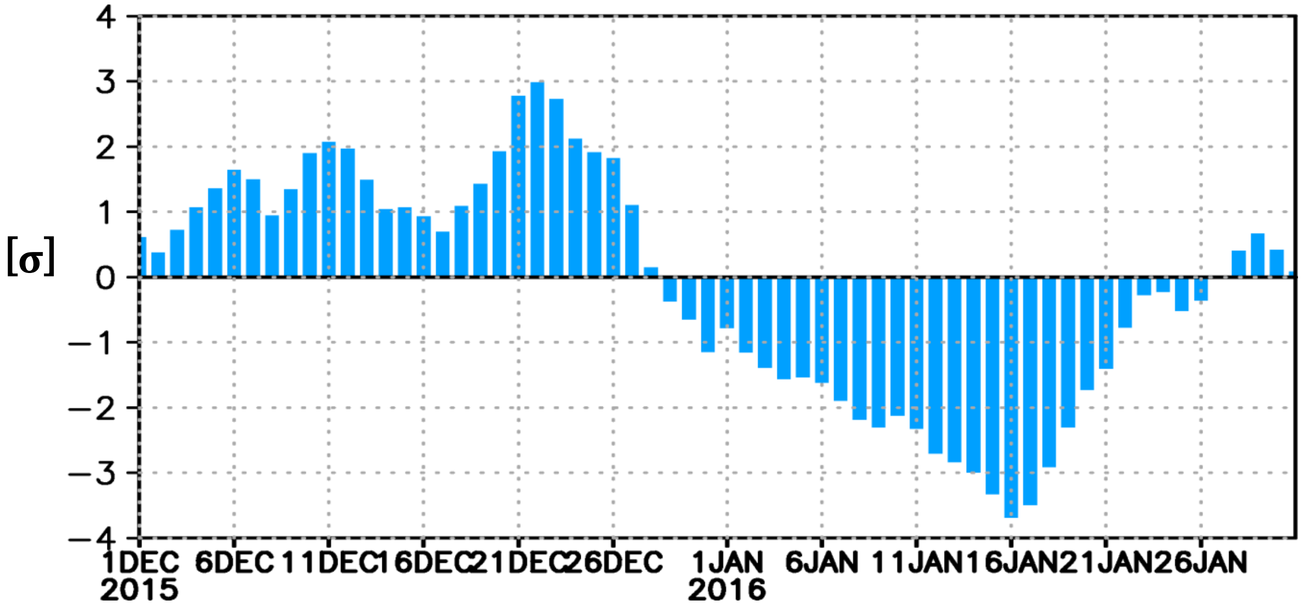

Figure 1.

Daily Time series of AO index from December 1, 2015 to January 31, 2016.

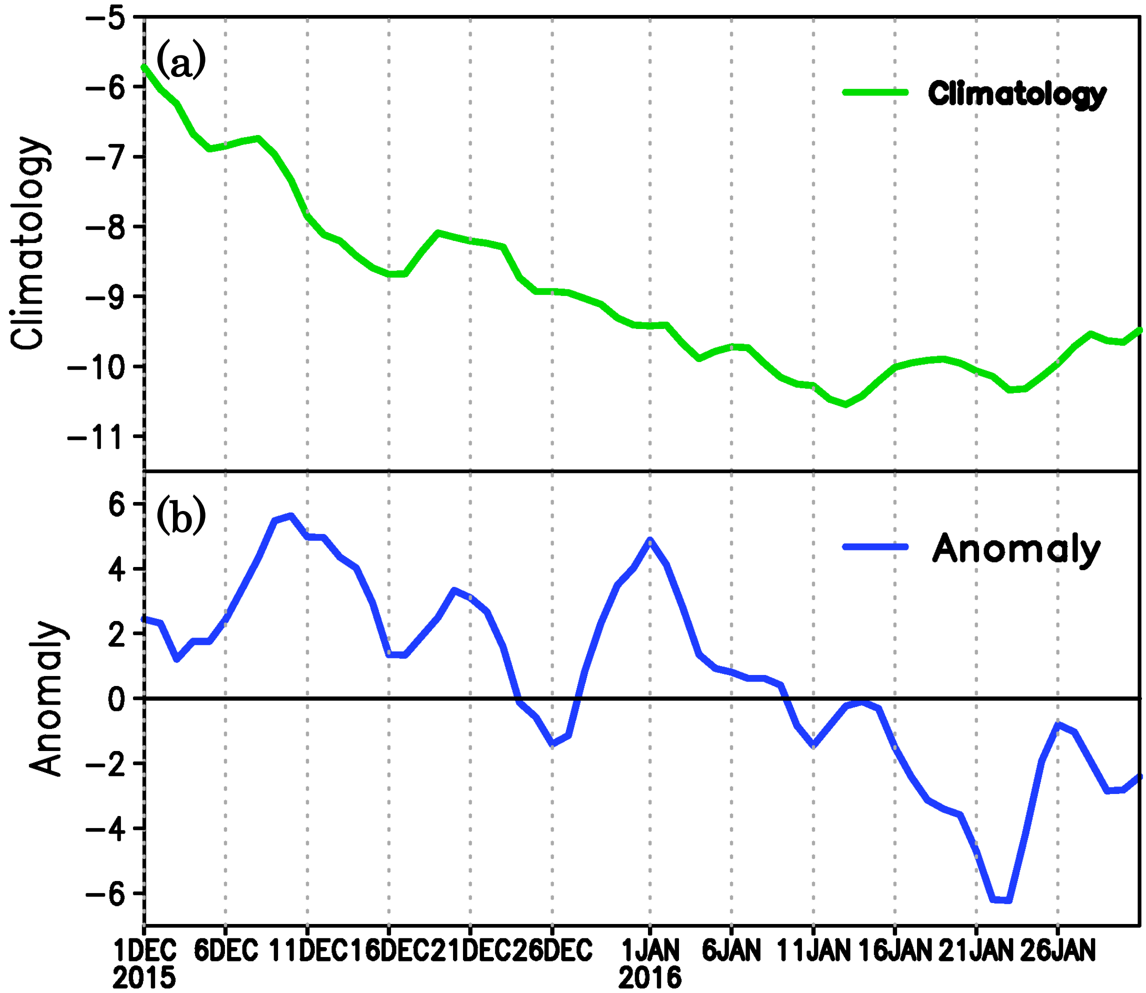

Figure 2.

Time series of daily East Asia temperature (°C) at 950 hPa from December 1, 2015 to January 31, 2016.

The green line indicated climatology (a) and blue line shows anomaly (b).

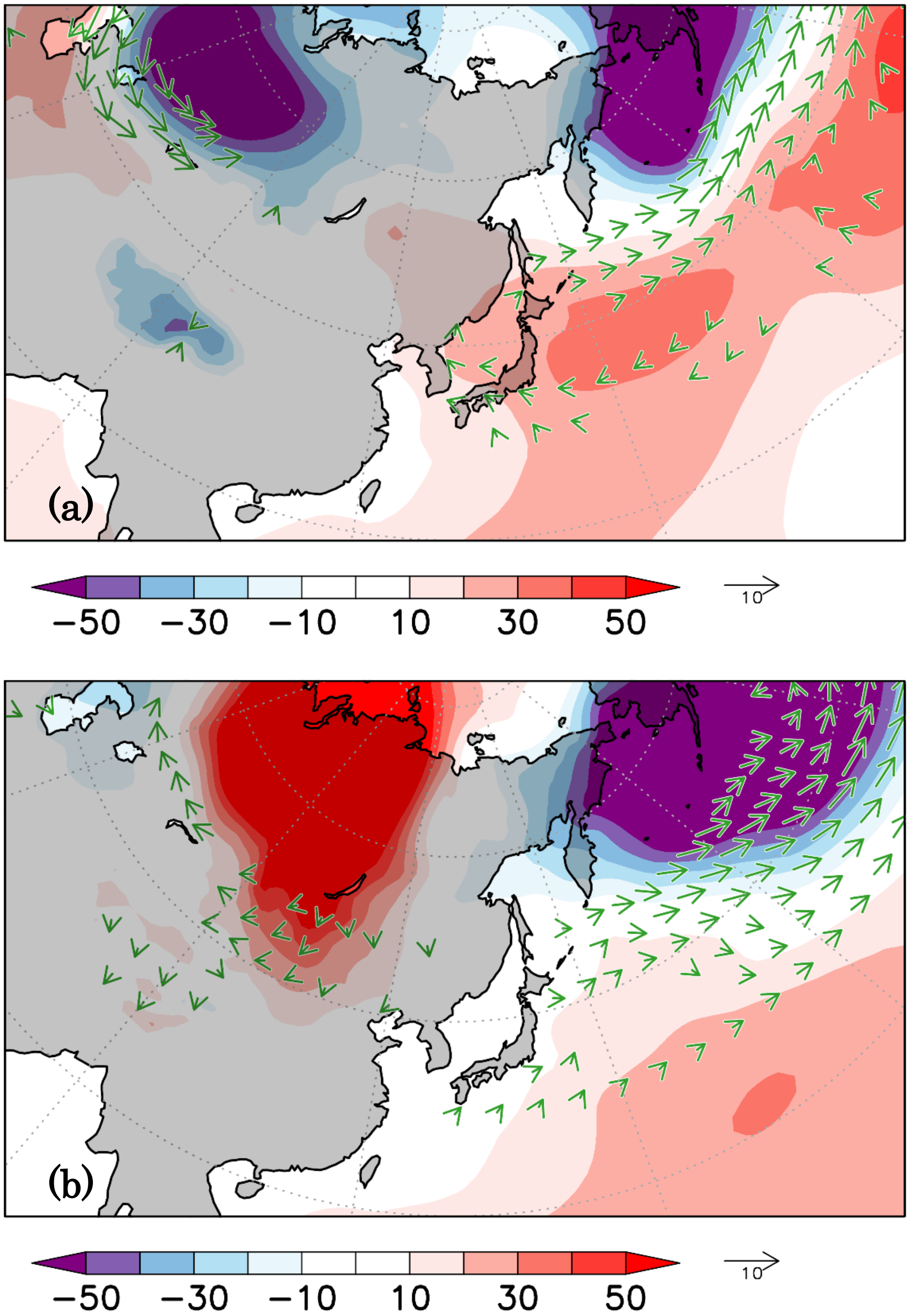

Figure 3.

Map of monthly mean geopotential height (m) anomaly (shaded) at 925 for December (a) and January (b). Vector indicates zonal wind and meridional wind (m/s) at 925 hPa for December and January.

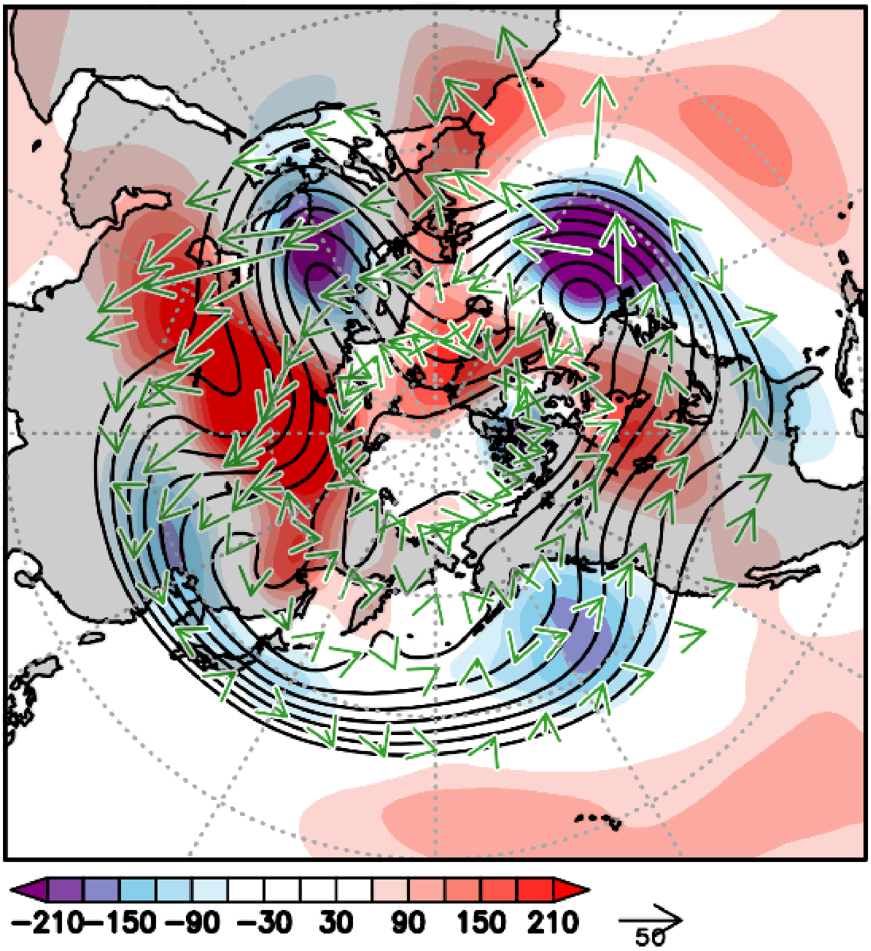

Figure 4.

300hPa geopotential height (m) field (contour) and anomaly (shade), vector of horizontal component indicated wave activity flux (m^2/s^2) from January 21, 2015 to 25 by Takaya and Nakamura (2001). Contour interval is 1000 m.

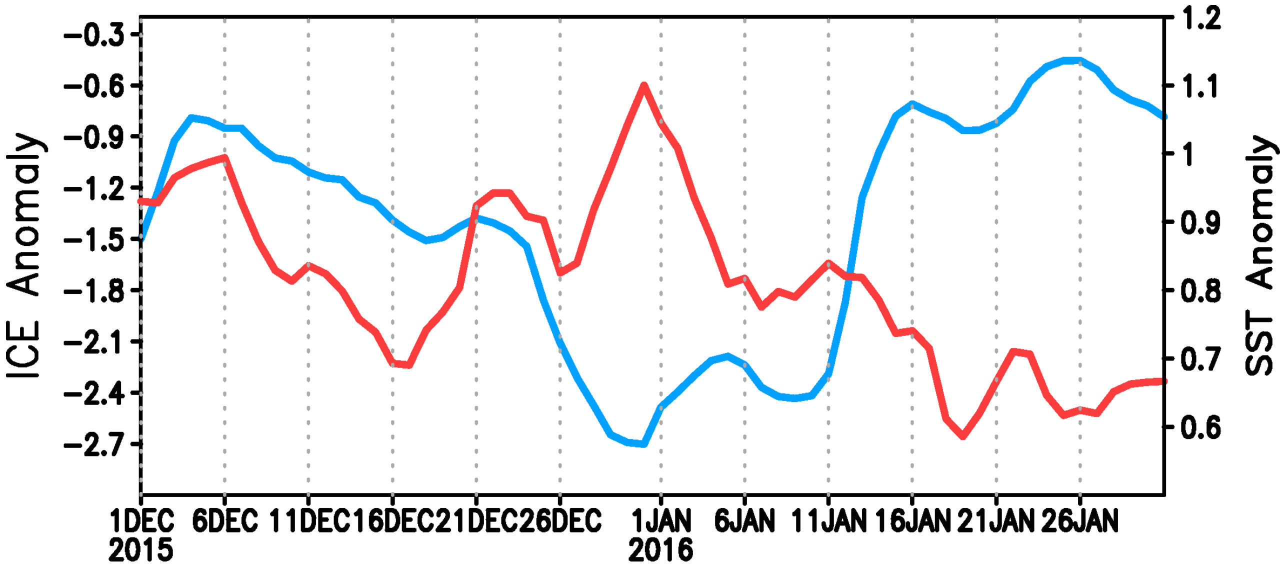

Figure 5.

Daily time series of BKS sea ice concentration and SST (℃) anomaly from December 1, 2015 to January 31, 2016. The blue line indicated sea ice anomaly and red line shows SST anomaly.

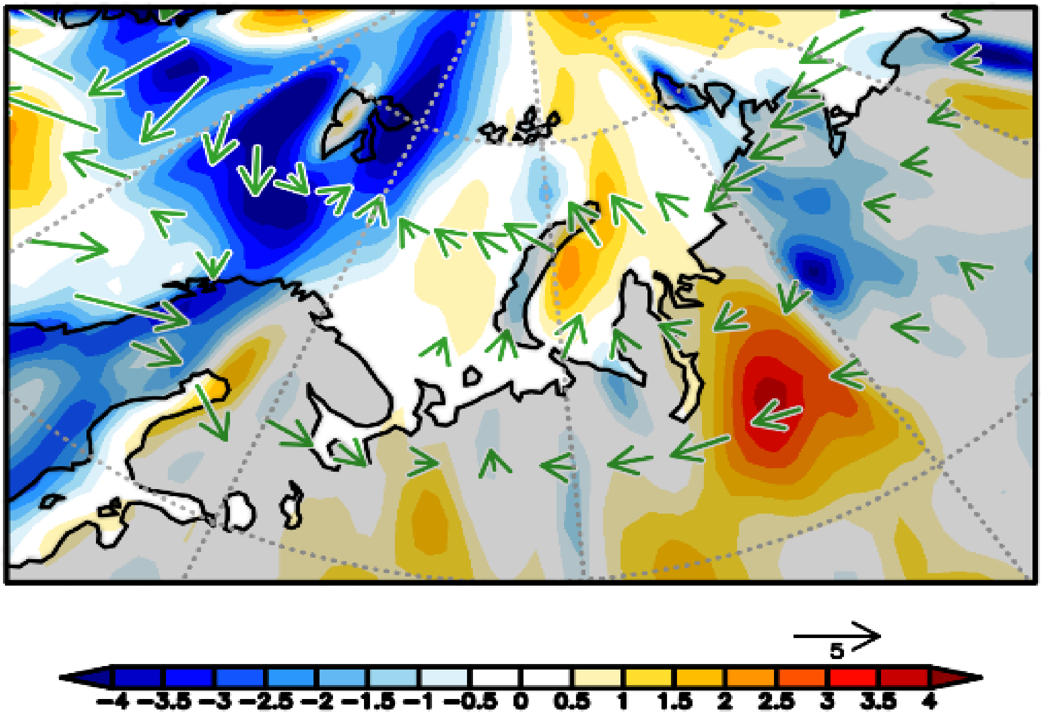

Figure 6.

Horizontal temperature advection ($-\boldsymbol{V_a} \cdot \nabla T_C$: ℃ /day) field (shade) and vector of horizontal component indicated wind anomaly (m/s) at 900 hPa from December 1, 2015 to 21.

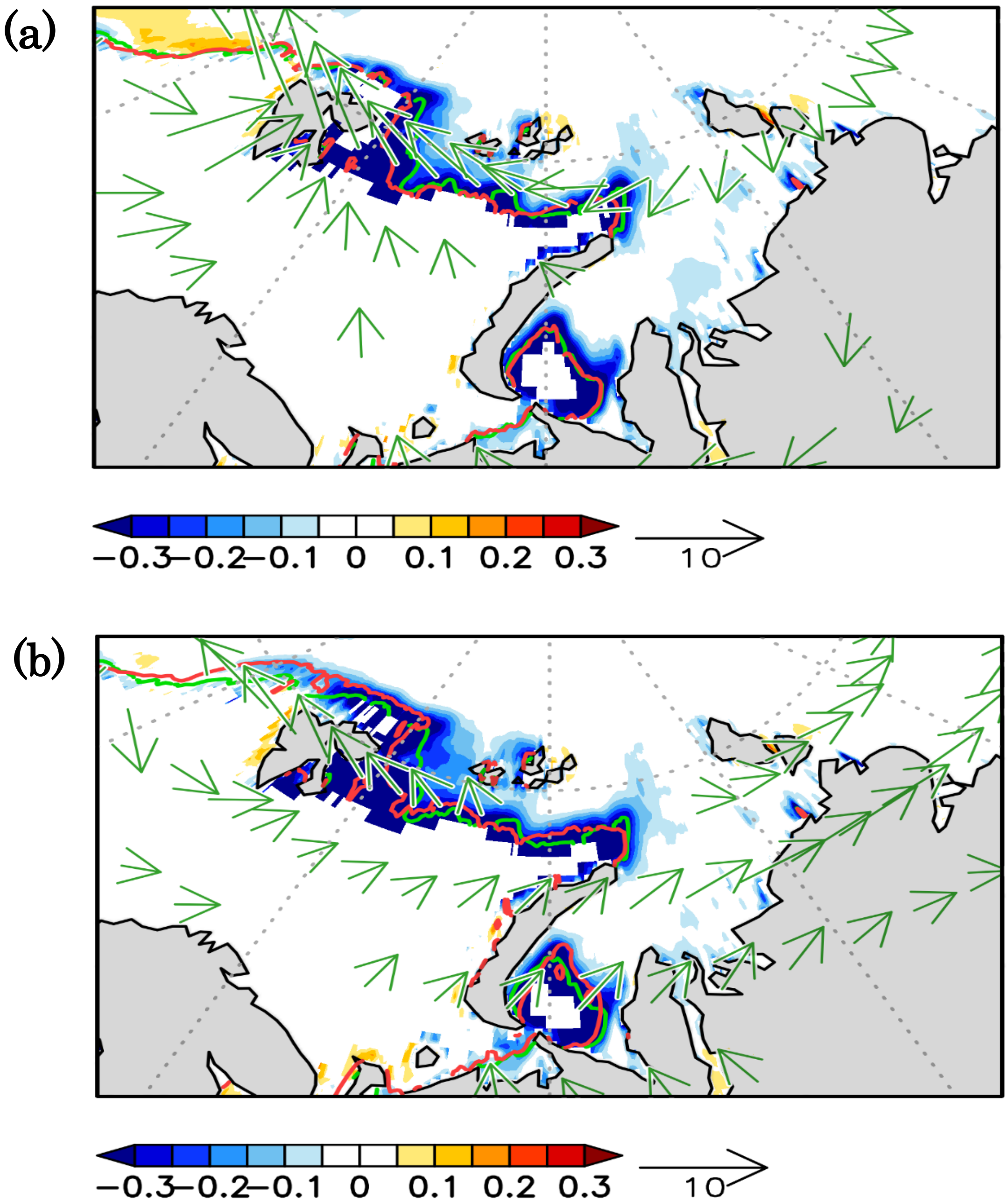

Figure 7.

(a) Horizontal wind anomaly (m/s) at 900 hPa from December 16, 2015 to 20, and sea ice concentration anomaly. Also, red line shows ice rim in December 16, 2015 and green line shows ice rim in December 20, 2015.

(b) It is similar to the above, in December 21, 2015 to 25. Also, red line shows ice rim in December 21, 2015 and green line shows ice rim in December 25, 2015.

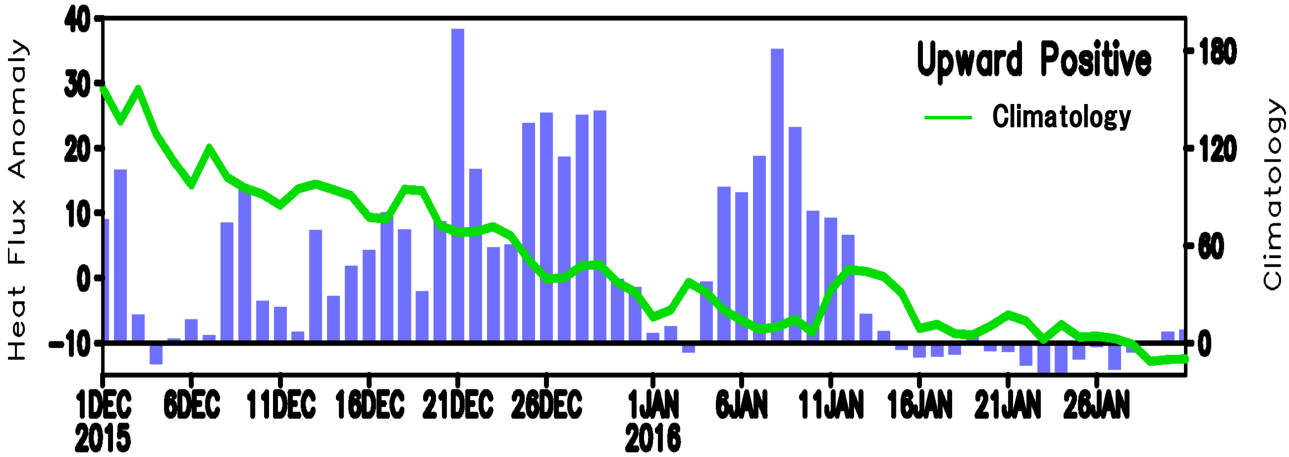

Figure 8.

Daily time series of BKS turbulent heat flux (Purple bar; W/m^2) anomaly and climatology (Green line; W/m^2) from December 1, 2015 to January 31, 2016.

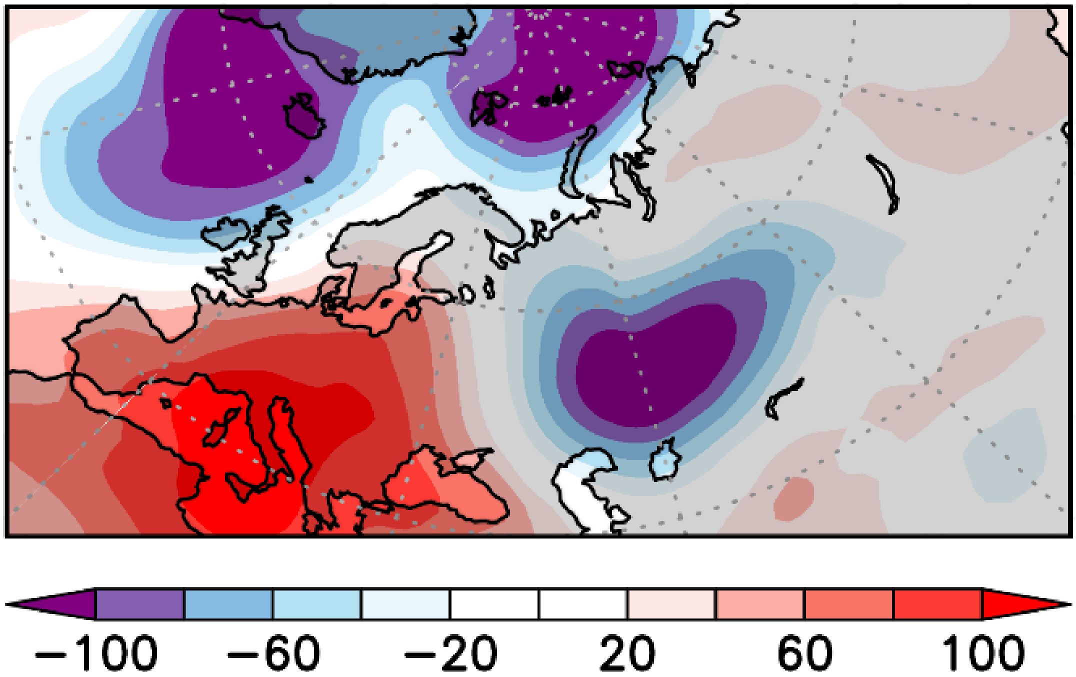

Figure 9.

Map of 10day mean geopotential height (m) anomaly at 1000 hPa from December 21, 2015 to 30.

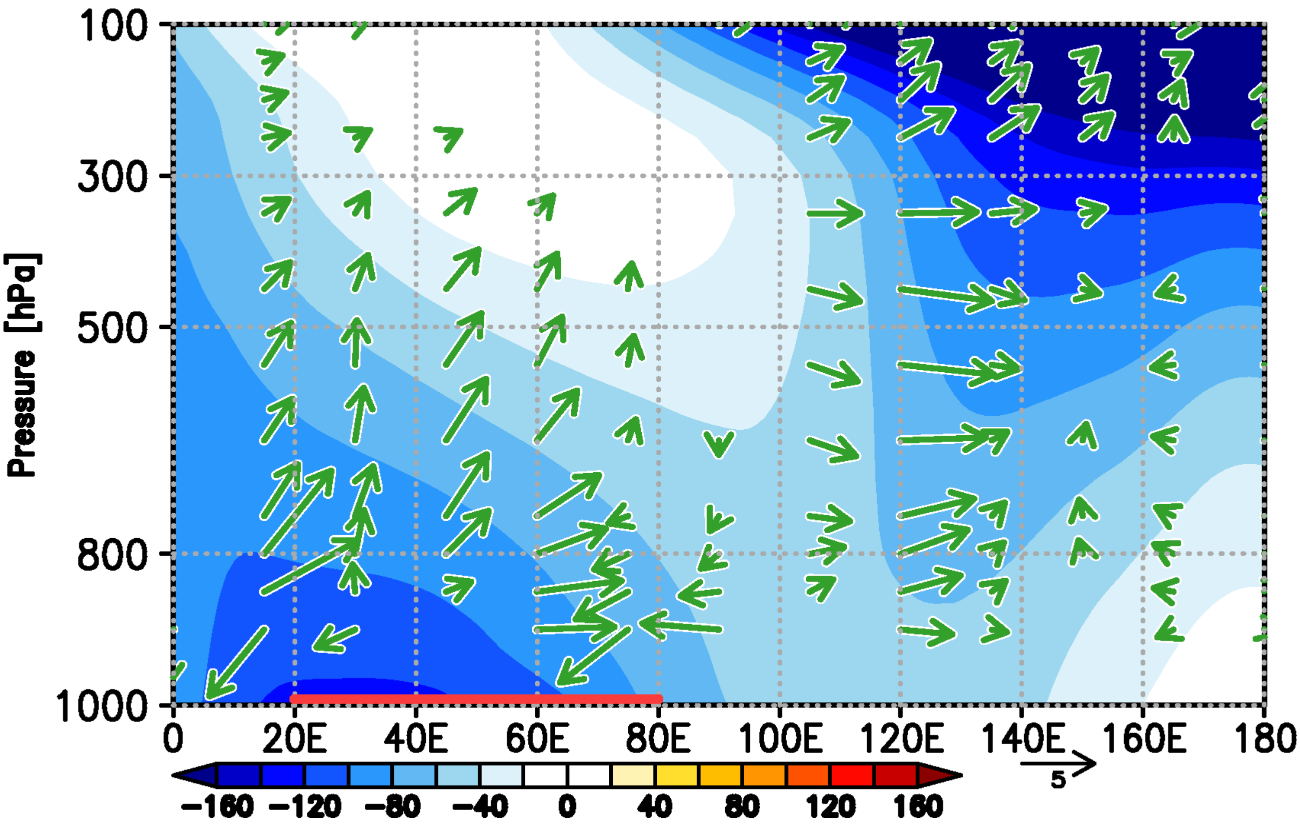

Figure 10.

Longitude-height cross section of geopotential height for northern latitude from 70°to 80°zonal mean anomalies (shade) and wave activity flux (vector) by Takaya and Nakamura 2001 from December 21, 2015 to 25. Red line shows BKS area during 20E and 80E.

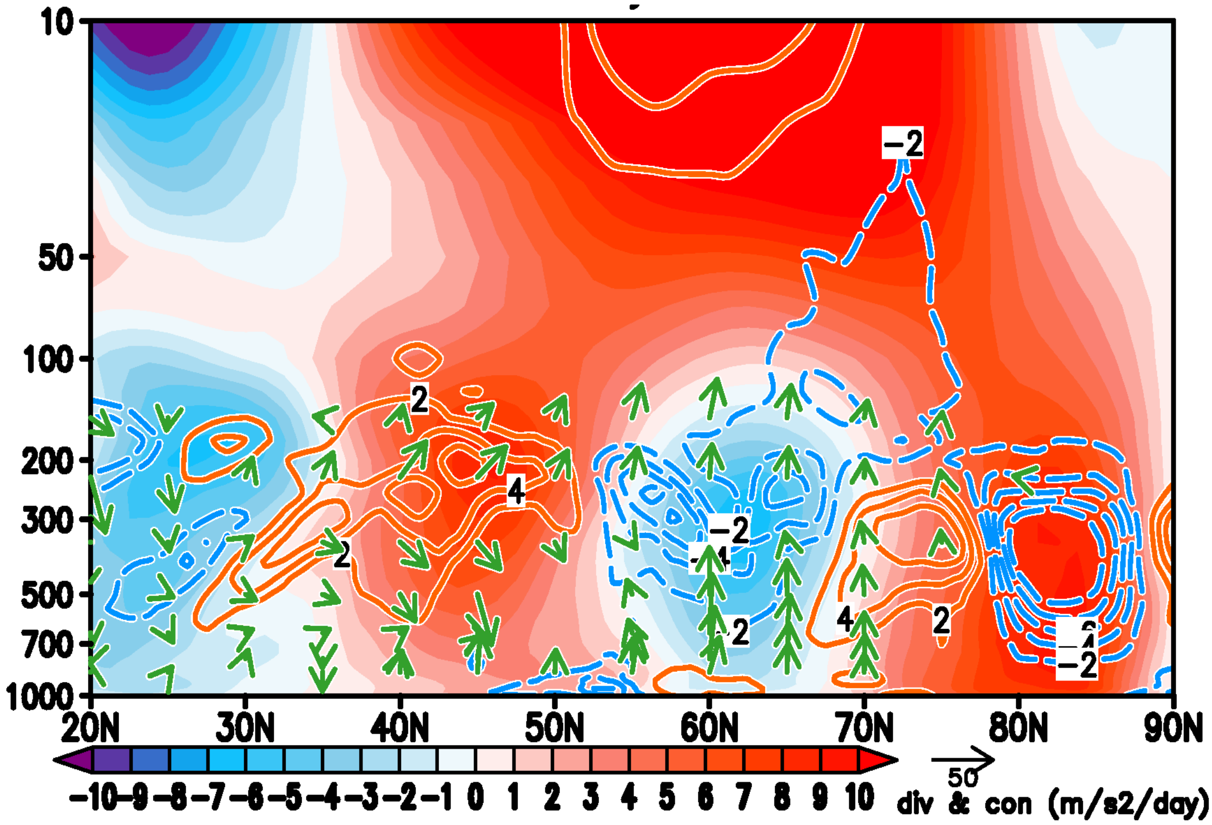

Figure 11.

Latitude-height cross sections of anomaly zonal-mean zonal wind (shade; m/s), EP-Flux (vectors; m^2/s^2), its divergence (red contour; m/s^2) and convergence (blue contour; m/s^2) from December 26, 2015 to 30. Contour interval is 2 m/s^2.

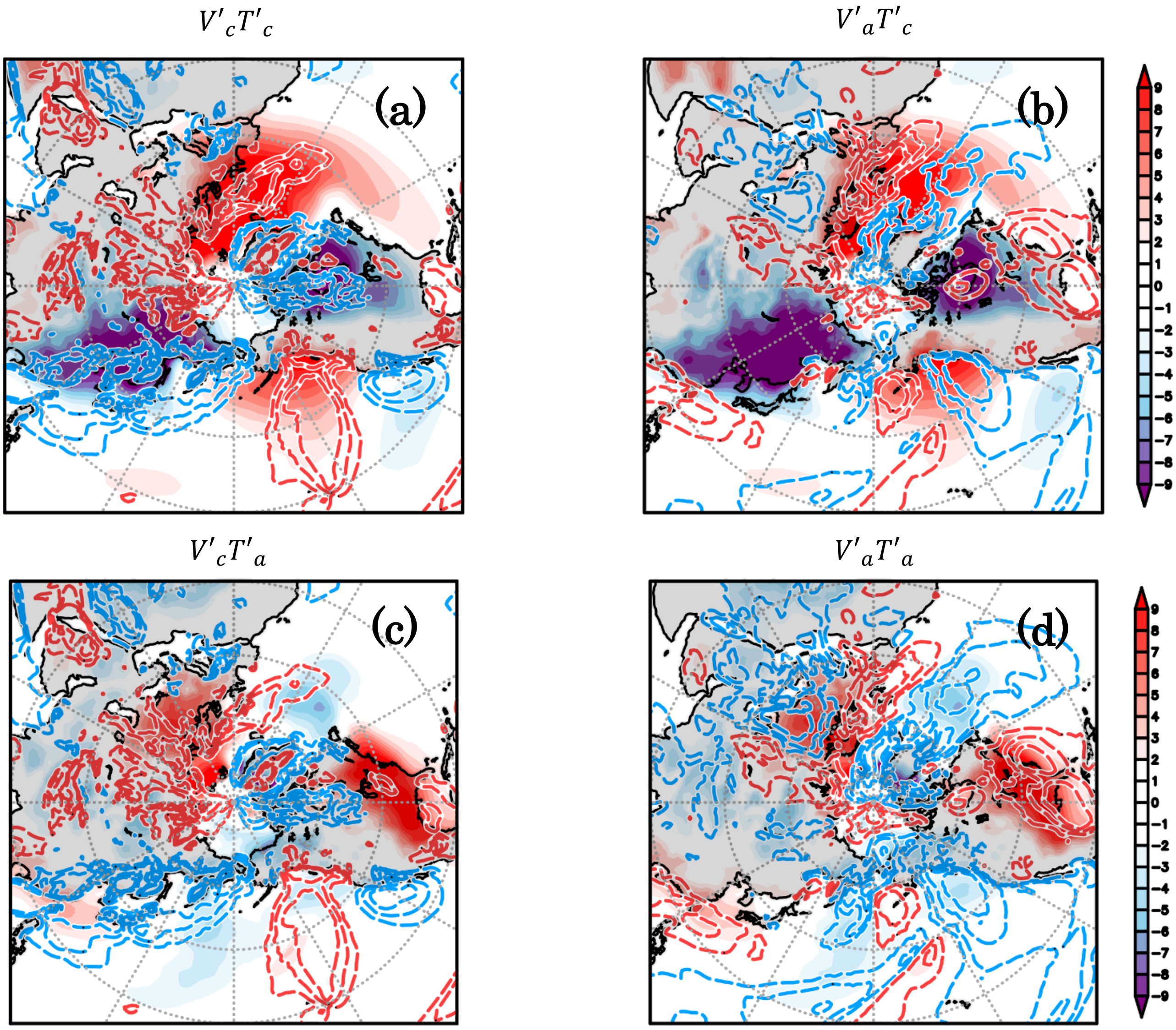

Figure 12.

Map of 5day mean poleward heat flux anomaly and climatology ($m \cdot$ ℃$/s$) at 950 hPa from December 26, 2015 to 30. Contours indicate meridional wind (m/s) and shade shows temperature (℃). (a) is $V'_cT'_c$, (b) $V'_aT'_c$, (c) $V'_cT'_a$, (d) $V'_aT'_a$. Contour interval is 2 m/s.

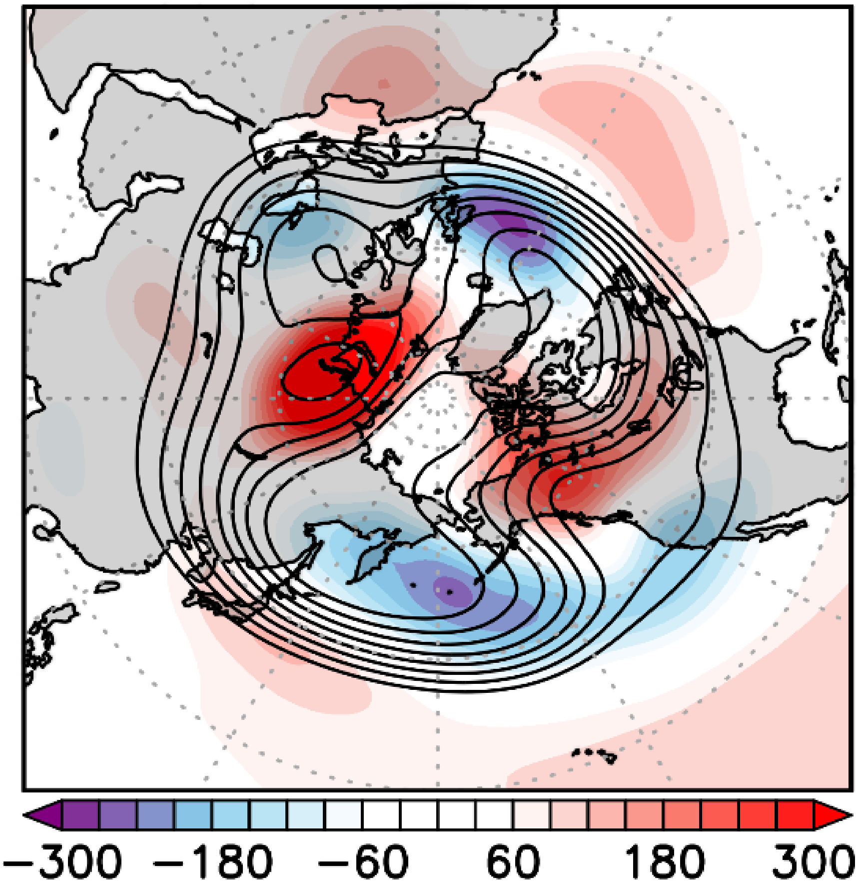

Figure 13.

Map of 10day mean geopotential height (m) anomaly (shade) and field (contour) at 300 hPa from December 31, 2015 to January 9, 2016. Contour interval is 1000 m.

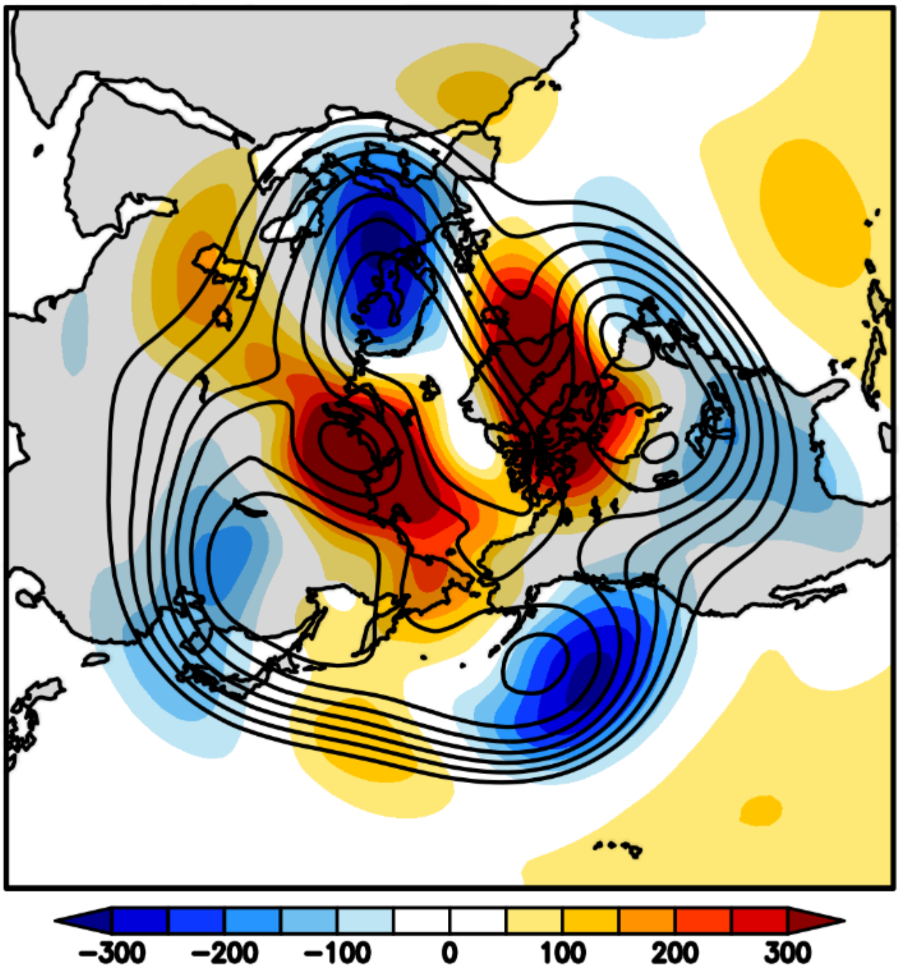

Figure 14.

Map of 5day mean geopotential height (m) anomaly (shade) and field (contour) at 300 hPa from January 10, 2016 to January 14. Contour interval is 1000 m.

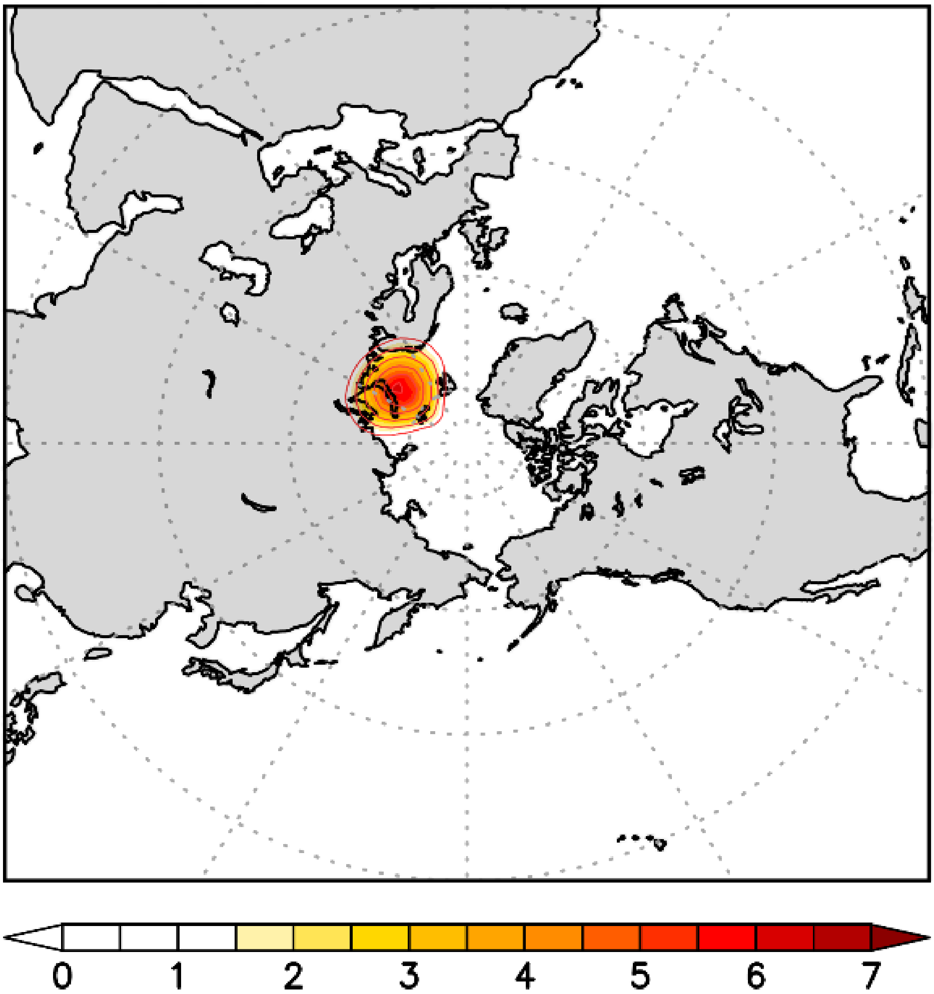

Figure 15.

In December climatology monthly mean field, it shows the location that gave the heat source to BKS in shade. Contour interval is 1.0 ℃/day.

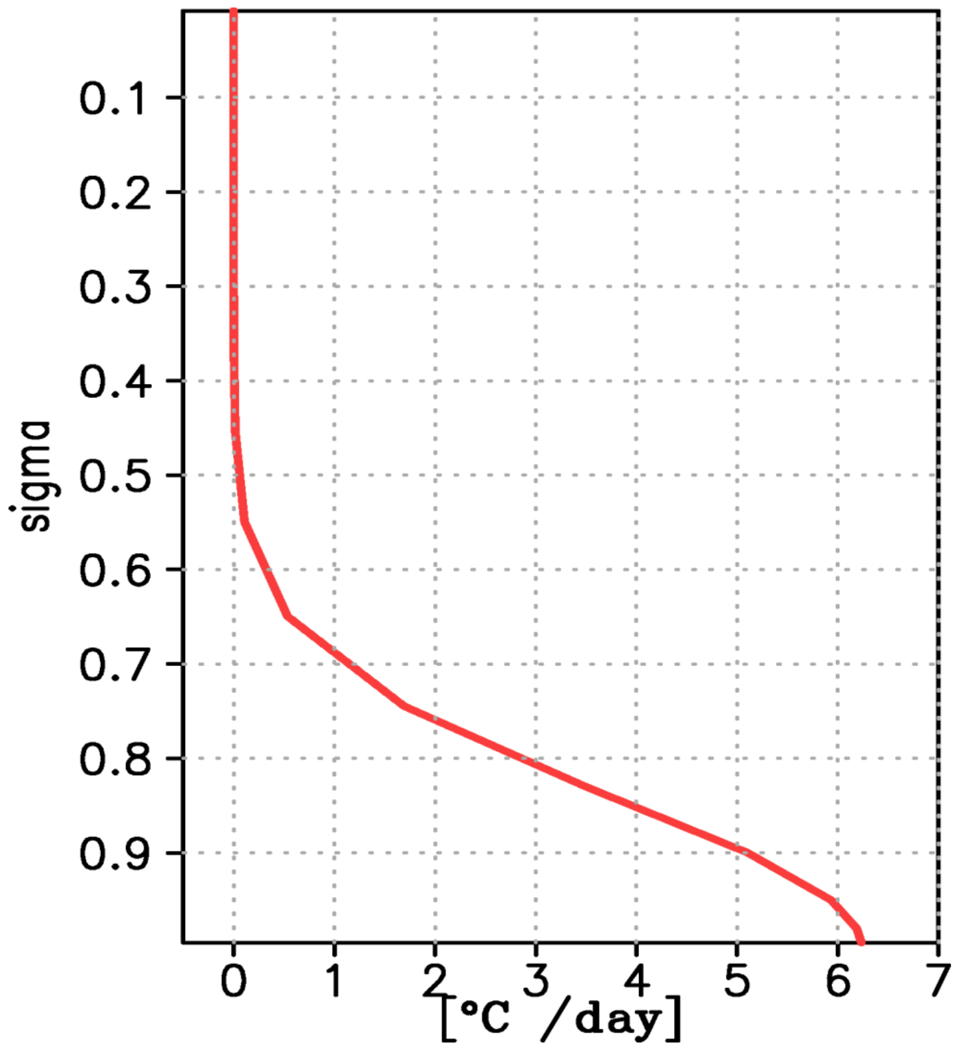

Figure 16.

°C/day -height cross sections of forcing value (°C/day) in Climatology. Vertically averaged diabatic heating from sigma levels 1.0-0.5.

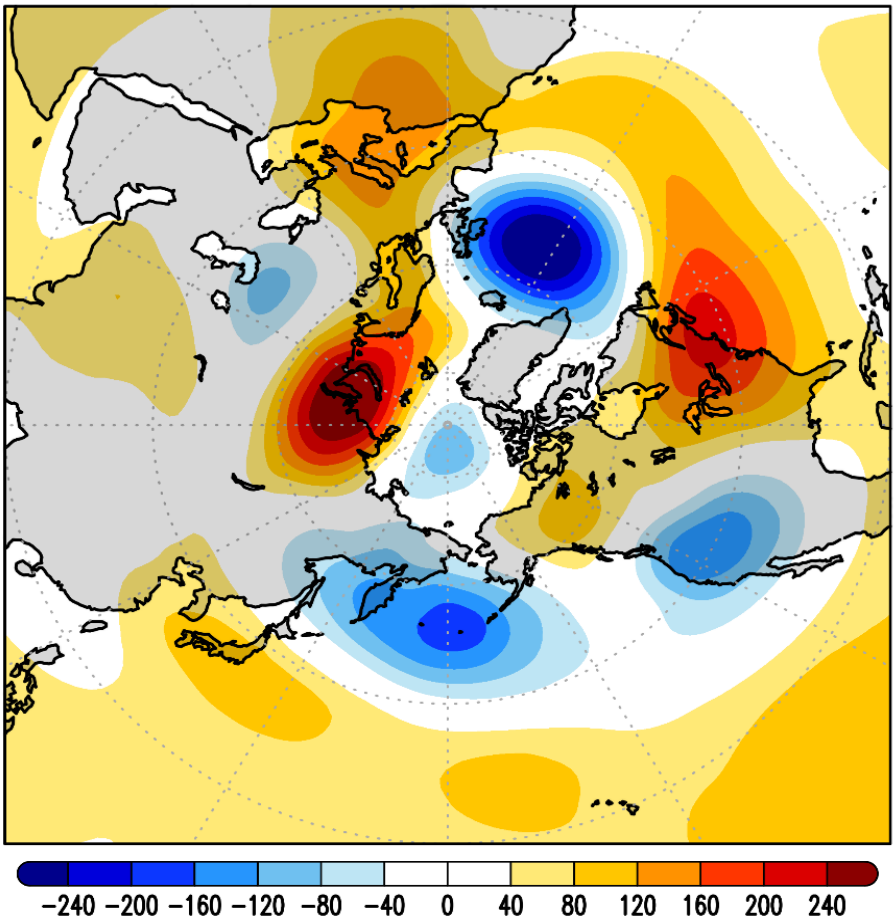

Figure 17.

Map of 21day mean geopotential height (m) anomaly (shade) at 300 hPa from December 21, 2015 to January 10, 2016.

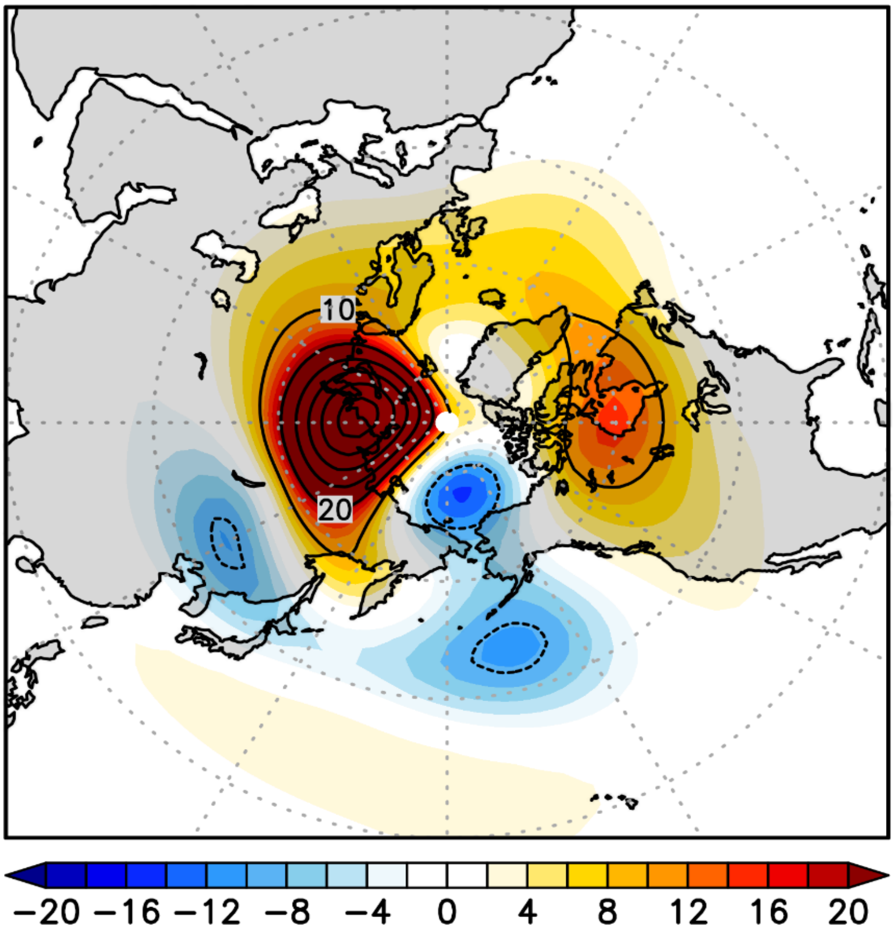

Figure 18.

Map of monthly mean geopotential height (m) vertically averaged diabatic heating at 300 hPa. Contour interval is 10 m.

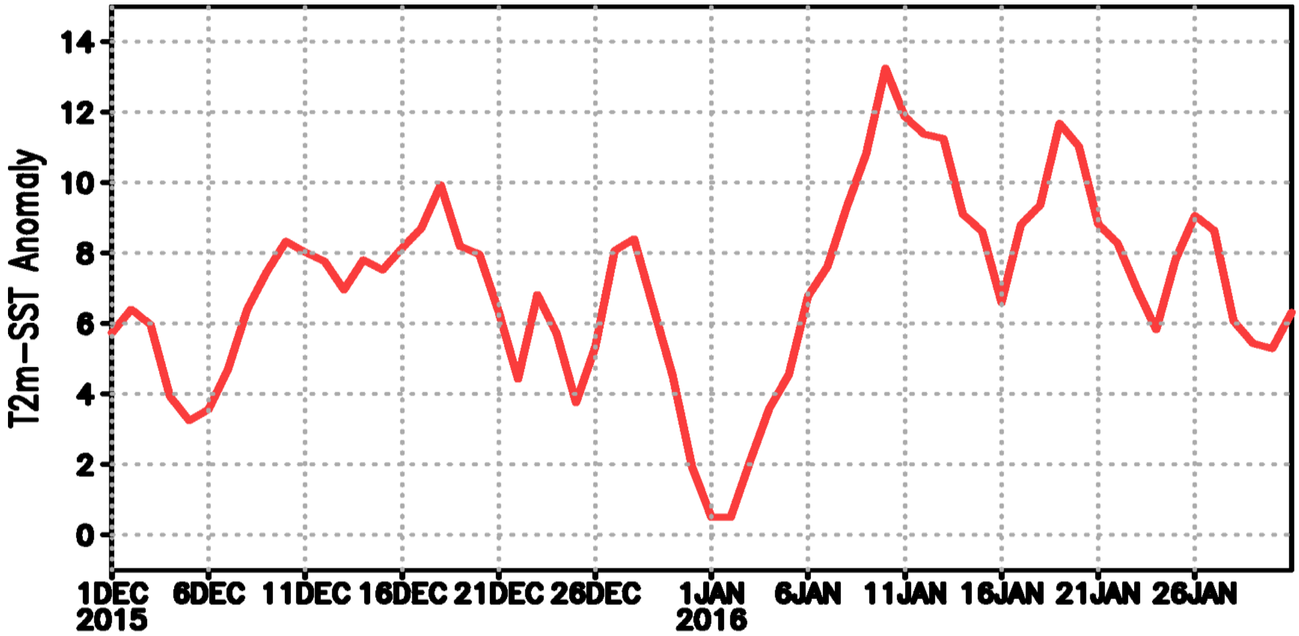

Figure 19.

Daily time series of BKS deviation from the SST (℃) to the 2 meter temperature (℃) during December and January.